

# N-body Study of Anisotropic Membrane Inclusions: Membrane Mediated Interactions and Ordered Aggregation

P. G. Dommersnes and J.-B. Fournier

Laboratoire de Physico-Chimie Théorique, E. S. P. C. I., 10 rue Vauquelin, F-75231 Paris Cédex 05, France  
(May 19, 2019)

We study the collective behavior of inclusions inducing local *anisotropic* curvatures in a flexible fluid membrane. The  $N$ -body interaction energy for general anisotropic inclusions is calculated explicitly, including multi-body interactions. Long-range attractive interactions between inclusions are found to be sufficiently strong to induce aggregation. Monte Carlo simulations show a transition from compact clusters to aggregation on lines or circles. These results might be relevant to proteins in biological membranes or colloidal particles bound to surfactant membranes.

Pacs numbers: 87.15.Kg, 64.60.Cn, 24.10.Cn

The interplay between structural features and  $N$ -body interactions is a general physical problem arising in many different contexts, e.g., crystals structure [1], magnetic atom clusters [3,4], colloids in charged fluids [2], polyelectrolyte condensation [5,6], and protein aggregation in biological membranes [7].  $N$ -body interactions can sometimes yield spectacular effects: non-pairwise summability of charge fluctuation forces can dramatically affect the stability of polyelectrolyte bundles [5]; three-body elastic interactions may induce aggregation of membrane inclusions, although two-body elastic interactions are repulsive [7]. In a system able to kinetically achieve equilibrium, the clusters formed are usually compact, however certain interactions may favor tenuous clusters. For instance, a recent  $N$ -body study has shown that above a critical strength of three-body interactions, the state of minimum energy is one in which all the particles are on a line [8]. It has also been observed recently that membrane mediated interactions can induce one-dimensional ring-like aggregates of colloidal particles bound to fluid vesicle membranes [9].

Manifolds embedded in a correlated elastic medium can impose boundary conditions, or modify the elastic constants. This usually gives rise to mean-field forces, which are due to the elastic deformation of the medium, and to *Casimir* forces, which are due to the modification of its thermal fluctuations. Such interactions are generally non pairwise additive [14]. The elastic interactions between defects in solids [10] or in liquid crystals [11] are well known examples of mean-field forces. Casimir forces exist between manifolds embedded in correlated fluids, such as liquid crystals and superfluids [12–14], or critical mixtures [15]. Another interesting example is the interaction between inclusions in flexible membranes [16,17]: it has been shown that cone shaped membrane inclusions experience both long range attractive Casimir interactions and repulsive elastic interactions. However, to our knowledge, there has been no rigorous study of the  $N$ -body interactions between membrane inclusions.

In this letter, we study the interplay between non pair-

wise additive membrane mediated interactions and the structure of inclusion aggregates. We calculate exactly the  $N$ -body interaction energy and the average shape of a membrane containing inclusions that are coupled to the membrane curvature. The two- and three-body interaction potentials are given explicitly. The *collective* behavior of identical inclusions is studied systematically by Monte Carlo (MC) simulations, using the full  $N$ -body interaction energy. We find no aggregation of isotropic inclusions, in contradiction with the prediction of Ref. [7]. Inclusions with sufficiently high anisotropic curvature self-assemble into various structures: those imposing a weak mean-curvature prefer to assemble into compact clusters, but as the ratio between mean-curvature and anisotropic curvature increases, we observe a transition to branched clusters, and linear or circular chains. In these aggregates, the multi-body interactions are of the same order as the two-body interactions. Our results could be relevant to understanding the aggregation and organization of proteins in biological membranes, or colloidal particles bound to surfactant membranes [9].

Let us consider a system of  $N$  anisotropic inclusions embedded in a flexible fluid membrane, in which they are free to diffuse laterally. In many situations, the surface tension is negligible and the membrane shape is governed by the Helfrich curvature energy  $h_0 = \frac{1}{2}\kappa(c_1 + c_2)^2 + \bar{\kappa}c_1c_2$  [18], where  $c_1$  and  $c_2$  are the two local principal curvatures of the membrane,  $\kappa$  is the bending rigidity, and  $\bar{\kappa}$  the Gaussian modulus. For biological membranes,  $\kappa \sim 30T$ , while for surfactant membranes it can be as small as a few  $T$  ( $T$  will denote throughout the temperature in energy units). We model the membrane shape by a simple parametric surface  $(\mathbf{r}, u(\mathbf{r}))$ , where  $\mathbf{r}$  is a vector in the  $(x, y)$  plane and  $u(\mathbf{r})$  the normal displacement field along  $z$ . The total Gaussian curvature energy, which contributes only to boundary terms at infinity [18], can be discarded in our problem. To quadratic order, the bare membrane Hamiltonian can be written as

$$\mathcal{H}_0 = \int d\mathbf{r} \frac{1}{2}\kappa (\nabla^2 u)^2. \quad (1)$$

Its correlation function,  $\langle u(\mathbf{0})u(\mathbf{r}) \rangle = (\beta\kappa)^{-1}G(\mathbf{r})$ , with  $\beta = 1/T$  the inverse temperature, is given by the Green function

$$G(\mathbf{r}) = (\nabla^4)^{-1}\delta(\mathbf{r}) = G(0) - \frac{1}{8\pi}r^2 \ln\left(\frac{L}{r}\right), \quad (2)$$

where  $L$  is a long wavelength cut-off, which is comparable with the size of the membrane.

Typical membrane inclusions have a central hydrophobic region spanning the hydrophobic core of the membrane, and two polar extremities protruding outside [19]. Assuming a strong orientational coupling between the lipids and the inclusion's boundary, which in general is not cylindrical, we model membrane inclusions as curvature sources [16], *point-like* as in [17]. Indeed, the size of the proteins is comparable with the short wavelength cut-off (the membrane thickness). Even large particles can be treated as point-like inclusions, provided one uses the curvature energy coarse-grained to the size of inclusions with its corresponding renormalized bending rigidity [20,21]. Hence, for an inclusion located at  $\mathbf{r}_n$ , we enforce the local condition

$$\nabla\nabla u|_{\mathbf{r}_n} = \mathbf{Q}_n \equiv \begin{pmatrix} K_n - J_n & 0 \\ 0 & K_n + J_n \end{pmatrix}, \quad (3)$$

where  $\nabla\nabla u$  is the curvature tensor of the membrane, formed by the second derivatives of  $u$ , and  $\mathbf{Q}_n$  is the curvature tensor locally imposed by the inclusion. Here,  $\mathbf{Q}_n$  is written in the frame of reference where it is diagonal,  $K_n$  being the mean-curvature and  $J_n$  the anisotropic curvature of the inclusion. While isotropic inclusions correspond to  $J_n=0$ , "hyperbolic" and wedge-shaped inclusions correspond to  $K_n=0$  and  $K_n=J_n$ , respectively. In the following, we may assume  $J_n \geq 0$  without loss of generality. We define the *orientation* of inclusion  $n$  by the direction of the lowest principal curvature, i.e.,  $K_n - J_n$ . The latter is defined modulo a rotation of angle  $\pi$ . Indeed, even if the inclusion bears an in-plane polarity, its coupling with the membrane curvature is apolar by symmetry.

Within this model, we can calculate the free energy  $\mathcal{F}$  of a membrane with  $N$  inclusions in a non perturbative way. Introducing an external field  $h(\mathbf{r})$ , eventually set to zero, the free energy is given by

$$\exp[-\beta\mathcal{F}] = \int \tilde{\mathcal{D}}[u] \exp\left[-\beta \int d\mathbf{r} u(\kappa\nabla^4)u + hu\right], \quad (4)$$

in which the constraints are implemented by delta functions in the measure

$$\tilde{\mathcal{D}}[u] = \mathcal{D}[u] \prod_{n=1}^N \delta(\nabla\nabla u|_{\mathbf{r}_n} - \mathbf{Q}_n). \quad (5)$$

This integral can be cast into a Gaussian form by replacing the delta functions by their Fourier representation

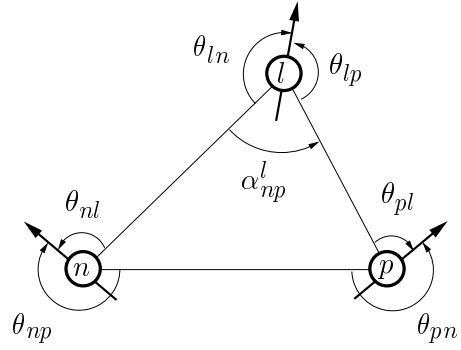


FIG. 1. Definition of the mutual orientations of three inclusions labeled  $n, m$ , and  $l$ . The angle  $\theta_{nl}$  is the orientation of inclusion  $n$  with respect to the line joining inclusions  $n$  and  $l$ , etc. All angles are defined modulo  $\pi$ , since any orientation and its reverse are equivalent.

(for details on this method, see, e.g., Ref. [14]). After integrating out the field  $u(\mathbf{r})$ , we obtain

$$\mathcal{F}[h] = \frac{T}{2} \ln(\det \mathbf{M}) + \frac{1}{2} \kappa \mathbf{b}' \mathbf{M}^{-1} \mathbf{b}'^t, \quad (6)$$

$$\mathbf{b}' = \mathbf{b} + \int d\mathbf{r} h(\mathbf{r}) \mathbf{c}(\mathbf{r}). \quad (7)$$

$\mathbf{M}$  is a  $3N \times 3N$  matrix formed by the blocks  $\mathbf{M}_{np} = \mathbf{D}^t \mathbf{D} G(\mathbf{r}_n - \mathbf{r}_p)$ , where  $\mathbf{D} = (\partial_x^2, \partial_x \partial_y, \partial_y^2)$ ;  $\mathbf{b}$  and  $\mathbf{c}(\mathbf{r})$  are  $3N$  vectors with blocks  $\mathbf{b}_n = [(\mathbf{Q}_n)_{11}, (\mathbf{Q}_n)_{12}, (\mathbf{Q}_n)_{22}]$  and  $\mathbf{c}_n = \mathbf{D} G(\mathbf{r} - \mathbf{r}_n)$ , respectively.

The average shape of the membrane is given by

$$\langle u(\mathbf{r}) \rangle = \left. \frac{\delta \mathcal{F}[h]}{\delta h(\mathbf{r})} \right|_{h=0} = \mathbf{c}(\mathbf{r}) \mathbf{M}^{-1} \mathbf{b}'^t. \quad (8)$$

Although not in explicit form, Eq. (6) allows to calculate *exactly* the  $N$ -body interaction, by inverting the matrix  $\mathbf{M}$  whose elements are simple functions of the distances between particles.  $\mathbf{M}$  and  $\mathbf{b}$  do not depend on  $T$ , therefore the first term in (6) corresponds to the fluctuation induced Casimir interaction, while the second term represents the mean-field elastic interaction.

Expanding the Casimir interaction  $\mathcal{F}^C = \frac{1}{2} T \ln(\det \mathbf{M})$  to fourth order in  $1/r_{np}$ , where  $r_{np} = |\mathbf{r}_n - \mathbf{r}_p|$ , yields

$$\mathcal{F}_4^C = -3T \sum'_{n,p} \frac{a^4}{r_{np}^4}, \quad (9)$$

in which the prime indicates restriction of the sum to different inclusions, and  $a$  is the short-wavelength cut-off (of the size of the inclusions) needed to regularize the derivatives of  $G(r)$  in  $r = 0$ . This fourth-order Casimir interaction is pairwise additive and corresponds exactly to the sum of the two-body interactions obtained in Refs. [16,17] for isotropic inclusions. It does not depend on the locally imposed curvature nor on the orientation of the inclusions (unlike the Casimir interaction between two rod-like inclusions [22]). This interaction is quite weak, since for

$r > 2a$  it is only a fraction of  $T$  and thus it is overwhelmed by diffusion.

Setting  $h = 0$  in the second term of (6) yields the mean-field elastic energy  $\mathcal{F}^{\text{mf}} = \frac{1}{2}\kappa \mathbf{b} \mathbf{M}^{-1} \mathbf{b}^t$ , which arises from the bending deformation of the membrane. To second order in  $1/r_{np}$ , we obtain (see Fig. 1 for the definition of the angles)

$$\mathcal{F}_2^{\text{mf}} = -4\pi\kappa \sum'_{n,p} \frac{a^4}{r_{np}^2} [2J_n J_p \cos(2\theta_{pn} - 2\theta_{np}) + K_n J_p \cos 2\theta_{pn} + K_p J_n \cos 2\theta_{np}]. \quad (10)$$

At this order, the mean-field interaction is pairwise additive. It depends on the imposed curvature tensors and on the orientations of the principal curvatures. To *fourth* order, the mean-field interaction includes both two-body interactions:

$$\mathcal{F}_{42}^{\text{mf}} = 2\pi\kappa \sum'_{n,p} \frac{a^6}{r_{np}^4} [(5 + \cos 4\theta_{np})J_n^2 + (5 + \cos 4\theta_{pn})J_p^2 + K_n^2 + K_p^2 + 4K_n J_n \cos 2\theta_{np} + 4K_p J_p \cos 2\theta_{pn}], \quad (11)$$

and *three-body* interactions:

$$\mathcal{F}_{43}^{\text{mf}} = \frac{4\pi}{3}\kappa \sum'_{n,p,\ell} \frac{a^6}{r_{n\ell}^2 r_{\ell p}^2} \left\{ J_n J_p [4 \cos(2\theta_{n\ell} + 2\theta_{p\ell} + 2\alpha_{np}^\ell) + 2 \cos 2\theta_{n\ell} \cos 2\theta_{p\ell}] + 2K_n J_p \cos(2\theta_{p\ell} + 2\alpha_{np}^\ell) + 2K_p J_n \cos(2\theta_{n\ell} + 2\alpha_{np}^\ell) + K_n K_p \cos 2\alpha_{np}^\ell \right\} + \text{perm.} \quad (12)$$

These terms can be attractive or repulsive, depending on the curvatures and orientations of the inclusions. Setting  $J_n = J_p = 0$  in (11), we recover the result of Refs. [16,17] for two isotropic inclusions; however, we also notice that the three-body interactions are in general of the same order as the two-body interactions.

Let us study the lowest-order mean-field interaction  $\mathcal{F}_2^{\text{mf}}$  between two identical anisotropic inclusions. Setting  $K_1 = K_2 = K$  and  $J_1 = J_2 = J$ , we may assume  $K \geq 0$  and  $J \geq 0$  without loss of generality. If  $K \neq 0$ , the energy is minimal when  $\theta_{12} = \theta_{21} = 0$ . The inclusions therefore tend to align their axis of smallest principal curvature (smallest in modulus) parallel to their separation vector. If  $K = 0$ , the energy is minimal whenever  $\theta_{12} = \theta_{21}$ . In both cases the interaction is attractive, contrary to the repulsive interaction found between two isotropic inclusions [16,17]. If  $\theta_{12} = 0$  and  $\theta_{21} \equiv \theta$  is arbitrary, the interaction is repulsive for  $\theta^* < |\theta| < \pi - \theta^*$ , where  $\cos 2\theta^* = -K/(K + 2J)$ , and otherwise attractive; the relation  $\pi/4 < \theta^* < \pi/2$  holds, where the lower limit corresponds to  $K = 0$ , and the upper limit to  $J \rightarrow 0$ . When  $\theta_{12} = \theta_{21} \equiv \theta$ , the interaction is also repulsive for  $\theta_c < |\theta| < \pi - \theta_c$  and attractive otherwise, with  $\cos 2\theta_c = -J/K$ . Again, we have  $\pi/4 < \theta_c < \pi/2$ , where the lower limit corresponds to  $J \rightarrow 0$  and the upper limit

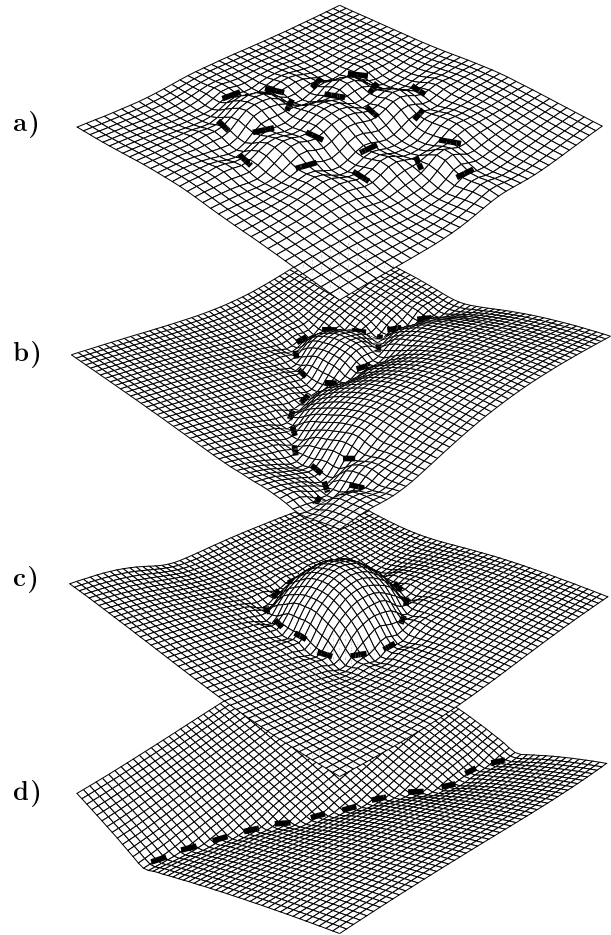


FIG. 2. Typical equilibrium aggregates obtained from MC simulation of  $N = 20$  identical inclusions. The corresponding values of  $(\bar{K}, \bar{J})$  are indicated in the phase diagram of Fig. 3. The mesh size corresponds to the microscopic cut-off  $a$ . The bars indicate the orientations of the inclusions.

to  $J = K$  (wedge-shaped inclusions). If  $J > K$  the interaction is always attractive when  $\theta_{12} = \theta_{21}$ .

As seen above, the lowest-order interaction between two identical anisotropic inclusions is already quite complex, however it is essentially attractive. Hence, one expects aggregation of the particles when the interaction energy overcomes the entropy of mixing. We noticed that the case  $K = 0$  is special, since the minimum energy is degenerate. Thus, one might expect compact clusters in this case, but for larger values of  $K$  it should become increasingly favorable to orient the inclusions along a common line joining them. To check these ideas, we have performed MC simulations on finite samples of  $N = 20$  identical inclusions. The positions and directions of principal curvatures were varied continuously, in order to avoid lattice artifacts. The energy was calculated from the  $N$ -body interaction (6), with  $h = 0$ , by numerically inverting the  $3N \times 3N$  matrix  $\mathbf{M}$ . When inclusions are close to contact, additional short-range interactions

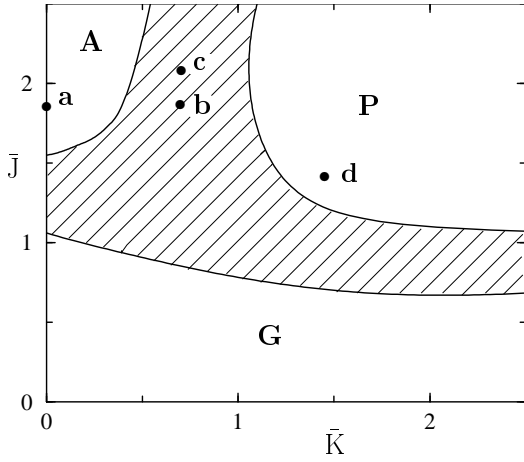


FIG. 3. Phase diagram of identical anisotropic inclusions obtained by MC simulations for different values of the inclusions mean-curvature  $\bar{K}$  and anisotropic curvature  $\bar{J}$ . (G) gas phase, (A) compact aggregates, and (P) linear polymer-like aggregates. In the dashed region, we found branched and ring-like aggregates, or small clusters close to the gas phase.

should be taken into account [23]. To mimic them, we have added a *repulsive* hard-core potential of diameter  $4a$ . Obviously, in the case of attractive short-range interactions, we cannot predict the aggregate shapes within the present model.

We started the simulations with a low-density distribution of inclusions having both random positions and orientations, then we let the system equilibrate using  $\sim 10^7$  MC steps. The relevant dimensionless parameters are  $\bar{K} = (\kappa/T)^{1/2}Ka$  and  $\bar{J} = (\kappa/T)^{1/2}Ja$ . For weak anisotropy, i.e.,  $\bar{J} \lesssim 1$ , the interaction was either repulsive or too weakly attractive to induce aggregation; for  $\bar{J} \gtrsim 1$ , the interaction was sufficiently attractive for the inclusions to aggregate. For small  $\bar{K}$ , we obtained compact clusters of inclusions, inducing some kind of decorated “egg-carton” structure of the membrane (Fig. 2a). As  $\bar{K}$  increased, we found a transition from compact aggregates to polymer-like ones (Fig. 2d). Remarkably, we also found ring-like aggregates, featuring a budding mechanism (Fig. 2b,c). The boundaries between the different aggregates shapes are depicted in the phase diagram of Fig. 3. Performing simulations with  $N = 60$ , we observed relatively weak fluctuations of the linear aggregates, indicating a persistence length of several hundred of inclusions or more. This suggests that “polymers” made of wedge-shaped inclusions can acquire a persistence length in the micron range. Long-range order might exist in the form of parallel inclusion lines, since for a two dimensional object, the  $1/r^2$  interaction is marginally long-range.

So far, we have only considered systems of *identical* inclusions, however our simulations may easily be extended to the case of inclusions inducing different curvatures. It

would also be interesting to study the effect of the long-range anisotropic interactions in the situation of kinetically constrained aggregation. In the case of a film with surface tension, we found similar anisotropic interactions, but of shorter range  $\sim 1/r^4$  at lowest order [24].

We thank R. Bruinsma and J. Prost for useful discussions. P. G. D. was supported by the Research Council of Norway.

- 
- [1] V. F. Lotrich and K. Szalewicz, Phys. Rev. Lett. **79**, 1301 (1997).
  - [2] R. R. Netz and H. Orland, Europhys. Lett. **45**, 726 (1999).
  - [3] G. M. Pastor, R. Hirsch and B. Muhlschlegel, Phys. Rev. Lett. **72**, 3879 (1994)
  - [4] G. M. Pastor, R. Hirsch and B. Muhlschlegel, Surface Review and Letters **3**, 447 (1996).
  - [5] B.-Y. Ha and Andrea J. Liu, Phys. Rev. Lett. **81**, 011 (1998)
  - [6] R. Podgornik and V. A. Parsegian, Phys. Rev. Lett. **80**, 1560 (1998).
  - [7] K. S. Kim, J. Neu, and G. Oster, Biophysical Journal, **75**, 2274 (1998).
  - [8] G. Date, P. K. Ghosh, and M. V. N. Murthy, Phys. Rev. Lett. **81**, 3051 (1998).
  - [9] I. Koltover, J. O. Rädler, and C. R. Safinya, Phys. Rev. Lett. **82**, 1991 (1999).
  - [10] L. D. Landau and E. M. Lifshitz, *Theory of Elasticity* (Pergamon Press, New York, 1987).
  - [11] P. G. de Gennes and J. Prost, *The Physics of Liquid Crystals* (Academic, New York, 1993).
  - [12] A. Ajdari, L. Peliti, and J. Prost, Phys. Rev. Lett. **66**, 1481 (1991).
  - [13] H. Li and M. Kardar, Phys. Rev. Lett. **67**, 3275 (1991).
  - [14] H. Li and M. Kardar, Phys. Rev. A. **46**, 6490 (1992).
  - [15] M. E. Fisher and P. G. de Gennes, C. R. Acad. Sci. Ser. B **287**, 207 (1978)
  - [16] M. Goulian, R. Bruinsma, and P. Pincus, Europhys. Lett. **22**, 145 (1993); Comment: J.-B. Fournier and P. G. Dommersnes **39**, 681 (1997).
  - [17] J. M. Park and T. C. Lubensky, J. Phys. I (France) **6**, 1217 (1996).
  - [18] W. Helfrich, Z. Naturforsch. **28 C**, 693 (1973).
  - [19] Lodish H. et al., *Molecular Cell Biology* (Scientific American Books, New York, 1995).
  - [20] W. Helfrich, J. Phys. (Paris), **46**, 1263 (1985).
  - [21] L. Peliti and S. Leibler, Phys. Rev. Lett. **54**, 1690 (1985).
  - [22] R. Golestanian, M. Goulian, and M. Kardar, Europhys. Lett. **33**, 241 (1996); Phys. Rev. E **54**, 6725 (1996).
  - [23] J.-B Fournier, Europhys. Lett. **43**, 725 (1998), and references therein.
  - [24] P. G. Dommersnes and J.-B. Fournier, to be published.